The Role of Arg46 and Arg47 of Antithrombin in Heparin Binding†

Véronique Arocas,‡ Susan C. Bock,§ Steven T. Olson,|| and Ingemar Björk*,‡

Department of Veterinary Medical Chemistry, Swedish University of Agricultural Sciences, Uppsala Biomedical Center, Box 575, SE-751 23 Uppsala, Sweden, Departments of Medicine and Bioengineering, UUHSC−Pulmonary Division, University of Utah, Salt Lake City, Utah 84132, and Center for Molecular Biology of Oral Diseases, University of Illinois−Chicago, Chicago, Illinois 60612

Received March 24, 1999

ABSTRACT: Heparin greatly accelerates the reaction between antithrombin and its target proteinases, thrombin and factor Xa, by virtue of a specific pentasaccharide sequence of heparin binding to antithrombin. The binding occurs in two steps, an initial weak interaction inducing a conformational change of antithrombin that increases the affinity for heparin and activates the inhibitor. Arg46 and Arg47 of antithrombin have been implicated in heparin binding by studies of natural and recombinant variants and by the crystal structure of a pentasaccharide−antithrombin complex. We have mutated these two residues to Ala or His to determine their role in the heparin-binding mechanism. The dissociation constants for the binding of both full-length heparin and pentasaccharide to the R46A and R47H variants were increased 3−4-fold and 20−30-fold, respectively, at pH 7.4. Arg46 thus contributes only little to the binding, whereas Arg47 is of appreciable importance. The ionic strength dependence of the dissociation constant for pentasaccharide binding to the R47H variant showed that the decrease in affinity was due to the loss of both one charge interaction and nonionic interactions. Rapid-kinetics studies further revealed that the affinity loss was caused by both a somewhat lower forward rate constant and a greater reverse rate constant of the conformational change step, while the affinity of the initial binding step was unaffected. Arg47 is thus not involved in the initial weak binding of heparin to antithrombin but is important for the heparin-induced conformational change. These results are in agreement with a previously proposed model, in which an initial low-affinity binding of the nonreducing-end trisaccharide of the heparin pentasaccharide induces the antithrombin conformational change. This change positions Arg47 and other residues for optimal interaction with the reducing-end disaccharide, thereby locking the inhibitor in the activated state.

Antithrombin is a major physiological regulator of the coagulation system in plasma, preventing excessive clotting. It inhibits clotting proteinases, most importantly factor Xa and thrombin, by forming stable, inactive complexes with the enzymes (*1*−*3*). Antithrombin belongs to the serpin superfamily of proteins, the serine proteinase inhibitors of which all appear to inactivate their target enzymes by the same general mechanism. The inhibition is initiated by an attack by the proteinase of a reactive bond (Arg393−Ser394 in antithrombin), located in an exposed surface loop of the inhibitor. Most evidence indicates that this attack progresses as a normal proteolytic cleavage to the acyl-intermediate (*4*−*6*). At this stage, the strain on the loop is released as a result of the reactive bond being severed, and the N-terminal segment of the loop is partially or fully inserted into the main β-sheet, the A-sheet, of the serpin (*6*−*9*). By this insertion, the proteinase, which is covalently linked to the inserting part of the loop by an acyl bond, is moved from the initial recognition site on the inhibitor (*8, 9*), possibly as far as to the opposite pole of the protein (*9*), and is trapped in an irreversible complex (*3*).

The sulfated polysaccharide heparin acts as a powerful anticoagulant by greatly (up to 4000-fold) accelerating the rate of inhibition of target proteinases by antithrombin (*3*). This effect depends on the binding of a specific pentasaccharide sequence of heparin to the inhibitor (*10*−*12*). The dissociation constant for the binding of heparin species having this sequence, denoted high-affinity heparin, to the predominant, fully glycosylated α-form of antithrombin in plasma is $(1-2) \times 10^{-8}$ M at pH 7.4 and ionic strength 0.15. The binding occurs in two steps and involves an initial weak interaction of heparin with antithrombin, followed by a conformational change of the inhibitor. This conformational change is essential for the increased rate of inactivation of factor Xa, whereas the accelerating effect on thrombin inactivation is predominantly due to a bridging effect, arising from proteinase and inhibitor being brought together by binding to the same heparin chain (*3*).

The site on antithrombin to which heparin binds has been the focus of considerable research in recent years. Basic residues, in particular Arg47, Arg129, Lys125, and Lys114,

† This work was supported by Swedish Medical Research Council Grant 4212 and European Community Biomed 2 Grant BMH4-CT96-0937 (to I.B.), and by National Institutes of Health Grants HL30712 (to S.C.B.) and HL39888 (to S.T.O.). V.A. was supported by l'Institut National pour la Santé et la Recherche Médicale (INSERM) and by an EMBO fellowship.

* To whom correspondence should be addressed at the Department of Veterinary Medical Chemistry, Swedish University of Agricultural Sciences, Box 575, SE-751 23 Uppsala, Sweden. Telephone: +46 18 4714191. Fax: +46 18 550762. E-mail: Ingemar.Bjork@vmk.slu.se.

‡ Swedish University of Agricultural Sciences.

§ University of Utah.

|| University of Illinois−Chicago.

10.1021/bi990686b CCC: $18.00
Published on Web 07/16/1999

have been implicated in the binding by studies of natural and recombinant variants of the inhibitor (*13*−*21*). The recent crystal structure of antithrombin in complex with a heparin pentasaccharide (*22*) confirmed these conclusions and defined the heparin-binding site in greater detail. The site was shown to be formed by the proposed basic residues and in addition by Arg46, Glu113, and possibly Lys11 and Arg13. The structure also indicated that the conformational change accompanying heparin binding involves an elongation of the D helix by 1.5 turns and the formation of a new 2-turn helix, the P helix, at right angles with the D helix (*22*). These changes cause a closing of the A-sheet and an expulsion of the partially inserted P14 and P15 residues of the reactive-bond loop from the A-sheet, which presumably is the cause of the increased reactivity of the loop with proteinases (*22*−*24*).

Although the heparin-binding site of antithrombin thus appears reasonably well defined, the importance of individual residues of this site for the affinity of the interaction with heparin and for the heparin-induced conformational change remains essentially unknown. Congenital antithrombin variants with mutations of Arg47 to Cys, Ser, or His are known to have an impaired heparin binding that is associated with thrombosis in the homozygous state (*13*−*15*, *17*), but the binding defect has not been quantified. Moreover, the Arg46 residue of antithrombin has been implicated in heparin binding only by the crystallographic studies. The aim of this work was therefore to elucidate the importance of Arg46 and Arg47 for the affinity and kinetics of binding of heparin to antithrombin and for the conformational change of the inhibitor. To this end, we have mutated Arg46 to Ala and Arg47 to His and characterized the resulting recombinant inhibitors, expressed in a baculovirus system. The affinity of both full-length heparin and pentasaccharide for antithrombin at pH 7.4 was decreased about 3-fold and 20-fold by the R46A[1] and R47H mutations, respectively, demonstrating a minor role of Arg46 in heparin binding and a substantial contribution of Arg47 to the binding. The affinity decrease caused by the Arg47 mutation was due to both a greater reverse rate constant of the conformational change step and a lower forward rate constant of this step, while the affinity of the initial binding step was essentially unaffected. Arg47 is thus not involved in the initial weak binding of heparin to antithrombin but is important for the heparin-induced conformational change of the inhibitor.

MATERIALS AND METHODS

Antithrombin Variants. Recombinant antithrombin variants were expressed in a baculovirus system as described earlier (*20*, *25*). The N135A antithrombin variant characterized previously (*25*, *26*) was used as a base molecule in this study. The R46A/N135A and R47H/N135A variants were produced by additional Arg46 to Ala and Arg47 to His substitutions, respectively. Mutant cDNAs were placed under control of the polyhedrin promoter and recombined into *Autographa californica* nuclear polyhedrosis virus DNA with the pFAST/DH10Bac Tn7-based transposition system from Life Technologies (Gaithersburg, MD). Sequences of antithrombin segments resynthesized during the PCR mutagenesis procedure were verified prior to transposition, and the mutations were reverified in virus from large-scale protein preparations by PCR amplification and sequencing.

The N135A and R46A/N135A variants were purified by heparin affinity chromatography at pH 7.4 on 5-mL Econo-Pac Heparin (Bio-Rad, Hercules, CA) or HiTrap Heparin (Amersham Pharmacia Biotech, Uppsala, Sweden) columns, as described previously (*20*, *25*). An initial purification of the R47H/N135A variant was done by the same procedure, but at pH 6 to increase heparin affinity (*14*, *17*). Nevertheless, this variant required further purification on a 1-mL HiTrap Heparin column, eluted with a 35-mL gradient from 0.02 to 3 M NaCl in 20 mM phosphate, pH 7.4, 0.1% (w/v) poly(ethylene glycol) 8000. Peak fractions from the chromatographies of the N135A, R46A/N135A, and R47H/N135A variants were pooled, dialyzed against 20 mM phosphate, pH 7.4, containing 0.1 M NaCl, 100 μM EDTA, and 0.1% (w/v) poly(ethylene glycol) 8000, and concentrated by ultrafiltration.

The purity of the antithrombin preparations was analyzed by SDS−PAGE and nondenaturing electrophoresis with the Laemmli buffer system (*27*). Total protein concentrations of the three variants were determined from the absorbance at 280 nm with the use of the molar extinction coefficient of plasma antithrombin, 37 700 M^{-1} cm^{-1} (*26*).

Proteinases. Human α-thrombin was a generous gift from Dr. John Fenton (New York State Department of Health, Albany, NY), and human factor Xa was prepared as described previously (*25*). The two preparations were >90% and ∼70% active, respectively, as shown by active-site titrations (*25*).

Heparins. Full-length heparin with high affinity for antithrombin and with an average molecular mass of ∼8000 Da (∼26 saccharide units) was isolated from commercial heparin as previously described (*12*, *28*, *29*). The antithrombin-binding heparin pentasaccharide (*11*) was a generous gift from M. Petitou (Sanofi Recherche, Toulouse, France). Concentrations of high-affinity heparin and pentasaccharide were determined by stoichiometric fluorescence titrations of plasma antithrombin with the saccharides (*12*).

Experimental Conditions. All experiments were performed at 25.0 ± 0.2 °C in 20 mM sodium phosphate, 100 μM EDTA, 0.1% (w/v) poly(ethylene glycol) 8000, adjusted to the required pH. NaCl was added to total ionic strengths of 0.15 to 0.6, the ionic strengths of the buffers in the absence of added salt, 0.025 and 0.05 at pH 6 and 7.4, respectively, being taken into account.

Stoichiometries of Thrombin Inhibition. Thrombin, at a constant concentration of 0.5 μM, was incubated at pH 7.4 and ionic strength 0.15 with increasing concentrations of the antithrombin variants to give inhibitor to enzyme molar ratios of 0 to ∼2. After 90 min, the residual enzyme activity was determined by diluting the incubation mixture 200-fold into a 100 μM solution of the chromogenic substrate S-2238 (Chromogenix, Mölndal, Sweden) and monitoring the initial rate of product formation by the absorbance at 405 nm. The residual activity at each inhibitor concentration was plotted against the molar ratio of inhibitor to enzyme, and the

[1] Abbreviations: H26, full-length heparin with high affinity for antithrombin and containing ∼26 saccharide units; H5, antithrombin-binding heparin pentasaccharide; K_d, dissociation equilibrium constant; k_{obs}, observed pseudo-first-order rate constant; k_{on}, overall association rate constant; k_{off}, overall dissociation rate constant; N135A, substitution of Asn135 by Ala; R46A, substitution of Arg46 by Ala; R47H, substitution of Arg47 by His; SDS−PAGE, sodium dodecyl sulfate−polyacrylamide gel electrophoresis.

apparent stoichiometry of inhibition was calculated by linear extrapolation of the data to the abscissa (*29*).

Fluorescence Titrations. Stoichiometries and affinities of full-length heparin or pentasaccharide binding to the antithrombin variants were measured by titrations monitored by the increase in the fluorescence of antithrombin tryptophan residues which accompanies the interaction (*12*, *29*−*31*). The titrations were done in an SLM 4800S spectrofluorometer (SLM Instruments, Rochester, NY) as described previously (*12*, *26*, *28*), with excitation at 280 nm and emission measured at 340 nm. Stoichiometries of full-length heparin binding were determined at pH 7.4 and ionic strength 0.15 with antithrombin concentrations, based on absorbance measurements, of 0.25−0.5 μM. Affinity titrations at pH 7.4 or 6.0 and different ionic strengths were done with antithrombin concentrations, obtained from the stoichiometry titrations, from 10-fold below to 3-fold above the measured K_d. In experiments at pH 6, antithrombin was diluted at least 40-fold in buffer of this pH just before the titrations. The results were analyzed by nonlinear least-squares fitting of the data to the equilibrium binding equation (*28*−*31*).

Kinetics of Heparin Binding. The rate of binding of full-length heparin or pentasaccharide to the antithrombin variants was measured at pH 7.4 and ionic strength 0.15 or 0.3 in a stopped-flow instrument (SX-17MV; Applied Biophysics, Leatherhead, U.K.), essentially as in earlier work (*12*, *26*, *32*). The experiments were done under pseudo-first-order conditions with heparin concentrations at least 10-fold higher than antithrombin concentrations, which were those derived from the heparin stoichiometry titrations. The interaction was monitored by the increase in protein fluorescence induced by heparin binding, with an excitation wavelength of 280 nm and an emission cutoff filter with ∼50% transmission at 320 nm. Values of k_{obs} were obtained by nonlinear regression fitting of the progress curves to a single exponential function. Four traces were typically averaged for each rate constant determination, and reported k_{obs} values are averages of at least four such determinations.

Kinetics of Proteinase Inactivation. The uncatalyzed rate of thrombin or factor Xa inhibition by the antithrombin variants, as well as the accelerating effect of full-length heparin or pentasaccharide on these reactions, was analyzed under pseudo-first-order conditions at pH 7.4 and ionic strength 0.15, essentially as described previously (*26*). Antithrombin variants (100 nM) were mixed with full-length heparin (0−5 nM) or pentasaccharide (0−7 nM), and proteinase (10 nM) was then added. At different times, aliquots were diluted 10-fold in buffer containing 100 μM S-2238 for thrombin or Spectrozyme FXa (American Diagnostica, Greenwich, CT) for factor Xa, and the residual proteinase activity was determined by measuring the initial rate of substrate hydrolysis at 405 nm. Polybrene was included at a concentration of 50 μg/mL in some analyses of thrombin inactivation in the absence of heparin as a check of heparin contamination of the antithrombin preparations. The data were fitted by nonlinear regression to a single-exponential function with an end point of zero activity to give k_{obs} (*29*). The second-order rate constants for the uncatalyzed and heparin-catalyzed antithrombin−proteinase reactions were obtained from these data as detailed earlier (*26*). The inhibitor concentrations used were those determined by the thrombin stoichiometric titrations described above.

RESULTS

Expression, Purification, and Homogeneity of Antithrombin Variants. The R46A and R47H antithrombin variants were expressed on an N135A background in this work. The substitution of Asn135 to Ala produces an antithrombin form lacking the oligosaccharide chain on this residue, analogous to the β-form that accounts for about 10% of the inhibitor in plasma (*25*, *26*, *33*). This form has an increased heparin affinity, which facilitates purification of variants with reduced heparin affinity (*25*, *26*). Moreover, the substitution eliminates a possible carbohydrate heterogeneity that may cause considerable heparin-binding heterogeneity (*27*, *34*−*36*).

Previous studies have shown that the natural R47H antithrombin variant has a higher affinity for matrix-linked heparin at pH 6 than at pH 7.4 (*14*, *17*). This property was used in the present work to improve the separation of the R47H/N135A variant from other proteins produced by the insect cells in which the recombinant inhibitor was expressed. However, a second heparin affinity chromatography at pH 7.4 was necessary to give a protein of high purity. In contrast, a single heparin affinity chromatography at this pH sufficed for the purification of the R46A/N135A and N135A variants. The R47H/N135A variant typically eluted from a 1-mL HiTrap Heparin column around 1.5 M NaCl at pH 7.4, whereas the R46A/N135A variant eluted around 2 M NaCl, and the N135A variant at greater than 2 M NaCl (*20*, *25*).

SDS−PAGE and nondenaturing electrophoresis of the N135A, R46A/N135A, and R47H/N135A variants showed that the three preparations were more than 95% homogeneous. The R46A/N135A and R47H/N135A variants had the same mobility as the N135A control in SDS−PAGE under both reducing and nonreducing conditions. However, they had a slightly higher mobility than the N135A control under nondenaturing conditions at alkaline pH, consistent with the loss of positive charge.

Stoichiometry of Heparin and Thrombin Binding. The stoichiometry of full-length heparin binding to the antithrombin variants was assessed by titrations, monitored by the increase in intrinsic fluorescence induced by the interaction, at pH 7.4, I 0.15, and high antithrombin concentrations. The stoichiometry ranged from 0.66 to 0.75 and from 0.64 to 0.82 for the N135A and R47H/N135A variants, respectively, for the two and three preparations, respectively, used throughout the work and was 0.56 for the single preparation of the R46A/N135A variant used. The interaction of heparin with the R46A/N135A and R47H/N135A variants resulted in the normal 35−40% enhancement of intrinsic tryptophan fluorescence observed for both plasma antithrombin and the N135A variant (*12*, *25*, *26*, *30*, *31*). Stoichiometries of thrombin binding to the variants were determined by measurements of the loss of thrombin activity against a chromogenic substrate and gave values comparable with those obtained for heparin binding. The preparations of the three variants thus contained some inactive, probably latent (*37*, *38*), inhibitor. Latent antithrombin, in which the reactive-bond loop is inserted into the A-sheet without prior reaction with a proteinase, does not inactivate proteinases and has a greatly reduced heparin affinity (*37*, *38*). This affinity is presumably comparable with that of reactive-bond-cleaved antithrombin, in which the loop is similarly inserted into the A-sheet, i.e., ≥1000-fold lower than the affinity of the intact

Table 1: Dissociation Equilibrium Constants, Bimolecular Association Rate Constants, and Dissociation Rate Constants for Full-Length Heparin and Pentasaccharide Binding to the N135A, R46A/N135A, and R47H/N135A Antithrombin Variants at 25 °C, pH 7.4, Ionic Strengths 0.15 and 0.3[a]

ionic strength	heparin form	antithrombin variant	K_d (nM)	$10^{-6} \times k_{on}$ ($M^{-1}\cdot s^{-1}$)	k_{off} (s^{-1})	calculated K_d (nM)[b]	calculated k_{off} (s^{-1})[c]
0.15	H26	N135A	~0.15[d]	154 ± 1	nd[e]		~0.02
		R47H/N135A	4.5 ± 2[d]	79 ± 2	0.5 ± 0.7	6 ± 9	0.35 ± 0.25
	H5	N135A	2 ± 1[d]	70 ± 2	nd		0.14 ± 0.07
		R47H/N135A	59 ± 2	28 ± 1	4 ± 0.5	150 ± 20	1.7 ± 0.2
0.3	H26	N135A	7 ± 1	23 ± 0.2	0.3 ± 0.1	13 ± 5	0.16 ± 0.03
		R46A/N135A	30 ± 1	nd	nd		
		R47H/N135A	130 ± 15	11 ± 0.2	2.4 ± 0.2	220 ± 20	1.4 ± 0.2
	H5	N135A	40 ± 4	28 ± 1	1.5 ± 0.4	54 ± 16	1.1 ± 0.2
		R46A/N135A	130 ± 5	nd	nd		
		R47H/N135A	580 ± 50	4.7 ± 0.2	9.5 ± 0.2	2000 ± 120	2.7 ± 0.4

[a] The K_d values are averages ± SE of at least three fluorescence titrations. The k_{on} and k_{off} values ± SE were obtained by linear regression of plots of k_{obs} vs heparin concentration, comprising 5−6 points in the 0.05−0.9 μM concentration range. [b] From k_{on} and k_{off}. [c] From K_d and k_{on}. [d] Estimated by linear extrapolation of values measured at higher ionic strengths (see Figure 1). [e] nd, not determined.

inhibitor (*39*). Active antithrombin concentrations used in subsequent studies of the interaction of the variants with heparin or proteinases were calculated from the measured stoichiometries of heparin and thrombin binding, respectively.

Heparin Affinity. Dissociation equilibrium constants, K_d, for the interaction of full-length heparin or pentasaccharide with the antithrombin variants were determined at pH 7.4, *I* 0.15 and 0.3, by fluorescence titrations similar to the stoichiometric titrations, but at lower antithrombin concentrations (Table 1). At *I* 0.15, most of the interactions were too tight to allow an accurate determination of K_d, and in these cases, the values for the R47H/N135A and N135A variants were instead estimated by extrapolation of data obtained at higher ionic strengths (see below). However, the K_d for all interactions could be measured at *I* 0.3.

The K_d values for binding of full-length heparin to the N135A variant (Table 1) agreed well with those obtained previously (*25*, *26*). However, the values for pentasaccharide binding were slightly higher than reported earlier (Table 1), possibly due to the use of different preparations of both pentasaccharide and the N135A variant. In agreement with previous results, full-length heparin bound somewhat more tightly than the pentasaccharide to the N135A variant (*25*, *26*). Both the R46A and R47H antithrombin mutations resulted in reduced heparin affinities, of similar magnitude for full-length heparin and pentasaccharide, compared with that of the N135A control. However, the affinity decrease was much more pronounced for the R47H/N135A variant (~30-fold at *I* 0.15 and 15−20-fold at *I* 0.3) than for the R46A/N135A variant (3−4-fold at *I* 0.3). Because of the low-affinity decrease caused by the R46A mutation and the small amounts of the R46A/N135A variant available, no further analyses of heparin binding to this variant were made.

Ionic Strength Dependence of Heparin Binding. The extent to which the reduction in full-length heparin and pentasaccharide affinity caused by the R47H mutation was due to loss of ionic or nonionic interactions was assessed by determination of K_d for the binding of the two heparin forms to the N135A and R47H/N135A antithrombin variants also at higher ionic strengths at pH 7.4. The ionic and nonionic contributions to the binding were evaluated from the dependence of the observed K_d values on sodium concentration with the aid of polyelectrolyte theory (*12*, *26*, *28*, *40*, *41*).

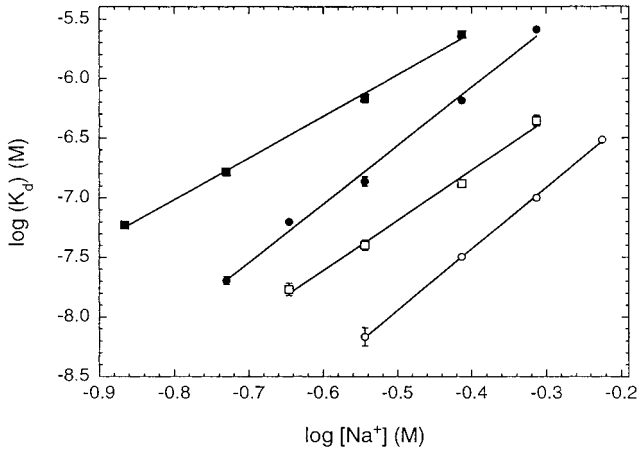

FIGURE 1: Sodium ion concentration dependence of dissociation equilibrium constants for full-length heparin and pentasaccharide binding to the N135A and R47H/N135A antithrombin variants at 25 °C, pH 7.4. (○) Full-length heparin, N135A; (□) pentasaccharide, N135A; (●) full-length heparin, R47H/N135A; and (■) pentasaccharide, R47H/N135A. Average values ± SE of at least three determinations are shown. Error bars not shown lie within the dimensions of the symbols. The solid lines represent linear regression fits.

Table 2: Ionic and Nonionic Contributions to Full-Length Heparin and Pentasaccharide Binding to the N135A and R47H/N135A Antithrombin Variants at 25 °C, pH 7.4[a]

heparin form	antithrombin variant	Z	log K_d'
H26	N135A	6.4 ± 0.1	−5.4 ± 0.1
	R47H/N135A	6.2 ± 0.3	−4.1 ± 0.1
H5	N135A	5.3 ± 0.2	−5.1 ± 0.1
	R47H/N135A	4.3 ± 0.2	−4.3 ± 0.1

[a] The number of ionic interactions (Z) involved in the binding of heparin to the antithrombin variants and the nonionic contribution (log K_d') to the binding were determined from the slopes and intercepts, respectively, of the plots in Figure 1. Errors represent ± SE obtained by linear regression.

Plots of log K_d against log [Na^+] were linear (Figure 1), the slopes and intercepts of these plots giving $Z\Psi$ and log K_d', respectively (Table 2), where Z is the number of ionic interactions involved in the binding, Ψ is the fraction of Na^+ that is bound per heparin charge and released on formation of the complex with antithrombin, and K_d' is the dissociation constant at 1 M Na^+, reflecting the affinity of the nonionic

interaction (*12*, *28*, *40*). The number of ionic interactions involved in the binding was calculated from a value for Ψ of 0.8, computed from the axial charge density of heparin (*28*). About five charges were shown to participate in the binding of pentasaccharide to the N135A variant, and about one more ionic interaction was found to be involved in full-length heparin binding, in agreement with previous work (*12*, *26*). The R47H substitution resulted in the loss of one charge interaction with the pentasaccharide. However, no comparable loss in charge interactions was apparent for full-length heparin binding.

The nonionic contributions to the binding of full-length heparin and pentasaccharide to the N135A variant were similar, as shown previously (*12*, *26*). However, these contributions were appreciably lower for the R47H/N135A variant. The decrease corresponded to an increase in K_d' of about 1 order of magnitude for both saccharides, although it was somewhat larger for full-length heparin than for the pentasaccharide.

Kinetics of Heparin Binding. The kinetics of binding of full-length heparin and pentasaccharide to the N135A and R47H/N135A antithrombin variants were studied under pseudo-first-order conditions in a stopped-flow instrument by continuous monitoring of the change in intrinsic fluorescence accompanying the binding. The observed fluorescence changes could be well fitted to a single-exponential function in all analyses.

At low concentrations of full-length heparin and pentasaccharide, ranging from 0.05 to 0.9 μM, the pseudo-first-order rate constant, k_{obs}, for the binding to the two variants at pH 7.4, *I* 0.15 and 0.3, increased linearly with the saccharide concentration, as shown previously for the N135A variant and plasma antithrombin (*12*, *26*, *32*). The slope and intercept of these plots gave the overall association rate constant, k_{on}, and the overall dissociation rate constant, k_{off}, respectively, for the binding (*12*, *26*, *32*) (Table 1). The k_{on} values could be measured with high accuracy at both *I* 0.15 and *I* 0.3, but most values of k_{off} were too low at *I* 0.15 to be determined with good precision. The values for the binding of full-length heparin and pentasaccharide to the N135A variant were similar to those measured previously (*26*) and showed that the weaker binding of the pentasaccharide was predominantly due to a higher k_{off}. The R47H mutation affected both k_{on} and k_{off} for the binding of the two saccharides. The k_{on} was thus lower and the k_{off} higher for the R47H/N135A variant than for the N135A variant at both ionic strengths and for both full-length heparin and pentasaccharide, consistent with the higher measured K_d values. The overall K_d was calculated as k_{off}/k_{on} when both these parameters could be measured (*12*) (Table 1). These calculated values and those measured by fluorescence titrations agreed within experimental error for the N135A variant, as in previous work (*26*), but the calculated values were up to ~3-fold higher than the measured ones for the R47H/N135A variant, the difference being larger for pentasaccharide than for full-length heparin binding.

The analyses of the heparin concentration dependence of k_{obs} for the binding of full-length heparin and pentasaccharide to the N135A and R47H/N135A antithrombin variants at pH 7.4, *I* 0.15, were extended to higher saccharide concentrations (Figure 2). The data for both antithrombin variants and both heparin forms were satisfactorily fit by a rectangular hyperbolic function, although the deviation from linearity was small for full-length heparin binding to the N135A variant. This behavior, shown previously for the binding of the two saccharides to both plasma and recombinant antithrombins (*12*, *26*, *32*, *41*), indicates that the binding occurs in two steps (Scheme 1). The initial step of this mechanism involves a weak, rapid-equilibrium binding of the two heparin forms to the inhibitor, which is followed by a conformational change of the protein that is responsible for the observed fluorescence change (*12*, *32*).

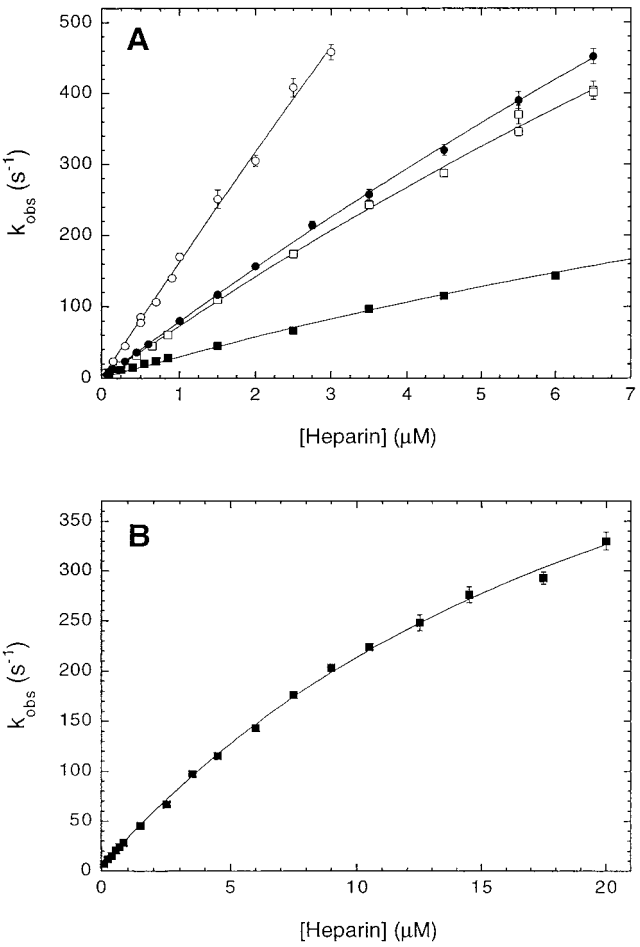

FIGURE 2: Heparin concentration dependence of observed pseudo-first-order rate constants for full-length heparin and pentasaccharide binding to the N135A and R47H/N135A antithrombin variants at 25 °C, pH 7.4, ionic strength 0.15. (A) (○) Full-length heparin, N135A; (□) pentasaccharide, N135A; (●) full-length heparin, R47H/N135A; and (■) pentasaccharide, R47H/N135A. (B) (■) Pentasaccharide, R47H/N135A. Note the different scales of the abscissa in (A) and (B). Average values ± SE of at least 16 individual measurements are shown. Error bars not shown lie within the dimensions of the symbols. The solid lines represent nonlinear regression fits to eq 1.

Scheme 1

$$AT + H \underset{}{\overset{K_1}{\rightleftharpoons}} AT{-}H \underset{k_{-2}}{\overset{k_{+2}}{\rightleftharpoons}} AT^{*}{-}H$$

In this scheme, AT is antithrombin, H is heparin, AT−H is the initial, weak complex, AT*−H is the final, tight complex, K_1 is the dissociation constant of the first binding step, and k_{+2} and k_{-2} are the forward and reverse rate constants, respectively, of the conformational change step. For this mechanism, k_{obs} varies with the total heparin concentration, $[H]_o$, according to the equation (*12*, *32*):

Table 3: Kinetic Constants of the Two-Step Mechanism in Scheme 1 for Full-Length Heparin and Pentasaccharide Binding to the N135A and R47H/N135A Antithrombin Variants at 25 °C, pH 7.4, Ionic Strength 0.15[a]

heparin form	antithrombin variant	K_1 (μM)	k_{+2} (s^{-1})
H26	N135A	≥10	≥3000
	R47H/N135A	36 ± 4	3000 ± 300
H5	N135A	28 ± 4	2100 ± 300
	R47H/N135A	23 ± 2	700 ± 30

[a] The dissociation equilibrium constant for the first step (K_1) and the forward rate constant for the second step (k_{+2}) of heparin binding to the antithrombin variants were obtained by fitting the data of Figure 2 to eq 1 by nonlinear regression. Errors represent ± SE obtained from these fits.

$$k_{obs} = \frac{k_{+2}[H]_o}{[H]_o + K_1} + k_{-2} \quad (1)$$

Moreover, k_{on} and k_{off}, measured at low saccharide concentrations, are equal to k_{+2}/K_1 and k_{-2}, respectively (*12*). In the nonlinear regression fits of the data of Figure 2 to eq 1 by which K_1 and k_{+2} were derived (Table 3), the values for k_{-2} were therefore fixed to those previously measured for k_{off}. Only lower limits of K_1 and k_{+2} for full-length heparin binding to the N135A variant could be evaluated, due to the nearly linear increase of k_{obs} with heparin concentration up to the highest measurable k_{obs}, in agreement with a previous study (*26*). The effect of the R47H mutation on the kinetic constants could thus be accurately quantified only for pentasaccharide binding. The values of K_1 and k_{+2} for this binding to the N135A variant were slightly different from those previously determined (*26*). K_1 for pentasaccharide binding was not detectably altered by the R47H mutation, whereas k_{+2} was reduced about 3-fold, accounting for the decrease in k_{on}.

pH Dependence of Pentasaccharide Binding. To assess whether the heparin binding defect caused by the R47H mutation could be reversed by increasing the positive charge on the histidine residue by lowering the pH (*14*, *17*), we measured the affinity of pentasaccharide binding to the N135A and R47H/N135A antithrombin variants at pH 7.4 and pH 6, *I* 0.4 (Table 4). The higher ionic strength was necessary to ensure accurate results at both pH values. As shown for plasma antithrombin (*41*), the affinity of the pentasaccharide for both the N135A and R47H/N135A variants was higher at pH 6 than at pH 7.4. However, the difference in K_d between pentasaccharide binding to the N135A and R47H/N135A variants was reduced from ~17-fold at pH 7.4 to ~4-fold at pH 6. This smaller difference indicates that the increased positive charge of the His residue at pH 6 to a large extent substitutes for the charge of the original Arg.

Rapid-kinetics studies at low pentasaccharide concentrations at *I* 0.4 showed that k_{on} for pentasaccharide binding to both antithrombin variants was higher and k_{off} lower at pH 6 than at pH 7.4 (Table 4), consistent with the higher affinities at the lower pH. The increase in k_{on} was much more pronounced for the R47H/N135A variant (~24-fold) than for the N135A variant (~3-fold), resulting in similar values of k_{on} for the two variants at pH 6. In contrast, the decrease in k_{off} for the R47H/N135A variant was much less marked (~3-fold), and the residual difference in affinity between this variant and the N135A control at pH 6 was completely accounted for by a difference in k_{off}.

Table 4: pH Dependence of Dissociation Equilibrium Constants, Bimolecular Association Rate Constants, and Dissociation Rate Constants for Pentasaccharide Binding to the N135A and R47H/N135A Antithrombin Variants at 25 °C, Ionic Strength 0.4[a]

pH	antithrombin variant	K_d (nM)	$10^{-6} \times k_{on}$ ($M^{-1}\cdot s^{-1}$)	k_{off} (s^{-1})
7.4	N135A	130 ± 6	11.1 ± 0.2	1.7 ± 0.1
	R47H/N135A	2300 ± 100	1.40 ± 0.04	15 ± 0.1
6	N135A	19 ± 3	32.9 ± 0.6	1.1 ± 0.3
	R47H/N135A	73 ± 8	33.5 ± 1.3	5 ± 0.9

[a] The K_d values are averages ± SE of at least three fluorescence titrations. The k_{on} and k_{off} values ± SE were obtained by linear regression of plots of k_{obs} vs heparin concentration, comprising 5−6 points in the 0.1−1.1 μM concentration range.

Table 5: Association Rate Constants for Uncatalyzed and Heparin-Catalyzed Reactions of the N135A and R47H/N135A Antithrombin Variants with Proteinases at 25 °C, pH 7.4, Ionic Strength 0.15[a]

proteinase	antithrombin variant	$10^{-3} \times k_{uncat}$ ($M^{-1}\cdot s^{-1}$)	$10^{-6} \times k_{H26}$ ($M^{-1}\cdot s^{-1}$)	$10^{-5} \times k_{H5}$ ($M^{-1}\cdot s^{-1}$)
thrombin	N135A	9.4 ± 0.4[b]	9.0 ± 0.5	nd[c]
	R47H/N135A	8.2 ± 0.5[b]	12.5 ± 0.4	nd
factor Xa	N135A	4.8 ± 0.2	1.2 ± 0.04	6.1 ± 0.2
	R47H/N135A	7.3 ± 0.3	1.4 ± 0.1	7.1 ± 0.2

[a] Second-order association rate constants for uncatalyzed (k_{uncat}), full-length heparin-catalyzed (k_{H26}), and pentasaccharide-catalyzed (k_{H5}) reactions of the antithrombin variants with proteinases were determined as described under Materials and Methods. The k_{uncat} values are averages ± SE of at least three determinations. Values of k_{H26} and k_{H5} ± SE were obtained by linear regression of plots of k_{obs} vs heparin concentration, comprising 4−6 points in the 0.1−7 nM concentration range. [b] Measured in the presence of 50 μg/mL Polybrene. 1.2-fold and 1.3-fold higher rate constants were measured in the absence of Polybrene for the N135A and R47H/N135A antithrombin variants, respectively, indicating minor heparin contaminations equivalent to less than 0.1 nM heparin, corresponding to a molar ratio to antithrombin of less than 0.001. Since this level of contamination was expected to insignificantly (<5%) affect rate constants for reactions with factor Xa, and since Polybrene appreciably (15−30%) enhances the rate of antithrombin−factor Xa reactions, the corresponding rate constants for factor Xa were measured without Polybrene. [c] nd, not determined.

Proteinase Inhibition. Second-order rate constants for the inhibition of thrombin and factor Xa by the N135A and R47H/N135A antithrombin variants were determined in the absence and presence of full-length heparin or pentasaccharide by discontinuous assays of residual proteinase activity (Table 5). The pentasaccharide enhancement of the rate of thrombin inhibition is minimal, less than 2-fold (*12*), and therefore was not investigated. Only minor differences were evident in the rate constants for both the uncatalyzed and the full-length heparin- or pentasaccharide-catalyzed inhibition of the two proteinases by the antithrombin variants.

DISCUSSION

A congenital antithrombin variant with a substitution of Arg47 to Cys was the first variant of the inhibitor reported to have a decreased affinity for heparin, an observation that led to the proposal that this residue participates in heparin binding (*13*). Subsequent findings of natural mutations of Arg47 to His or Ser also being associated with a decreased

heparin affinity reinforced this conclusion (*14*, *15*, *17*). The recent X-ray structure of a complex of antithrombin with a heparin pentasaccharide further supported the involvement of Arg47 in heparin binding and also implicated the neighboring Arg46 residue in this binding (*22*). In the present work, we have quantified the contribution of Arg46 and Arg47 to the binding of heparin by measurements of the affinity for full-length heparin and the heparin pentasaccharide of recombinant antithrombin variants in which these two residues had been mutated. Replacement of Arg46 by Ala was shown to cause a 3−4-fold decrease in the affinity of antithrombin for both heparin forms at pH 7.4, I 0.3. This observation confirms the contribution of Arg46 to heparin binding suggested by the X-ray structure, but shows that this contribution is minor. Therefore, no further analyses of the background to the decreased heparin affinity of this variant were made. In contrast, the R47H substitution resulted in a ∼30-fold decrease in antithrombin affinity for the two heparin forms at *I* 0.15, pH 7.4, and a ∼20-fold decrease at *I* 0.3, reflecting an appreciably larger contribution by Arg47 to heparin binding. The uncatalyzed and catalyzed rates of inhibition of thrombin and factor Xa were unaltered by the R47H mutation, indicating that the latter only affected the affinity of antithrombin for heparin and pentasaccharide and not the native or activated conformations of the inhibitor. The observed reductions in affinity correspond to a binding energy of 7−8.5 kJ·mol^{-1}, i.e., about 15% of the total free energy of binding of the two saccharides to the parent inhibitor. This contribution by Arg47 to heparin binding is sufficient to be of physiological importance, as individuals with homozygous mutations of this residue are at risk of developing thrombosis (*13*, *42*).

The reduced affinity of the R47H/N135A antithrombin variant for the heparin pentasaccharide at pH 7.4, where His is essentially uncharged, was due to the loss of both one charge interaction and nonionic interactions, as shown by the ionic strength dependence of the dissociation equilibrium constant, K_d. Arg47 thus establishes the expected electrostatic interaction with a negatively charged group in the pentasaccharide, presumably the carboxyl group on iduronic acid unit G suggested by the X-ray studies (*22*). However, it also contributes appreciable binding energy by nonionic interactions, which may be hydrogen bonds or hydrophobic interactions. The role of the charge interaction is further demonstrated by the considerably lower reduction in pentasaccharide affinity, compared with that of the control inhibitor, measured for the R47H/N135A variant at pH 6.0 than at pH 7.4. This observation shows that the increased positive charge of the His residue at the lower pH can substitute for that of the original Arg residue. Surprisingly, a comparable loss of a charge interaction at pH 7.4 was not apparent for binding of full-length heparin to the R47H/N135A variant from the ionic strength dependence of K_d. The decreased affinity for full-length heparin caused by the mutation was instead due only to a loss of nonionic interactions, which was somewhat larger than in the case of the pentasaccharide, thereby resulting in comparable reductions in affinity for the two saccharides. It is reasonable to conclude from the pentasaccharide findings that the charge interaction between Arg47 and the pentasaccharide region in full-length heparin also would be abolished by the mutation of this residue. The observed behavior therefore suggests that the R47H substitution allows full-length heparin to establish a compensating ionic interaction with antithrombin outside the pentasaccharide region, in addition to that presumably occurring with the Arg132−Lys136 region of the inhibitor (*12*, *22*, *43*).

The rapid-kinetics studies were consistent with both full-length heparin and pentasaccharide binding to the R47H/N135A antithrombin variant by the two-step, induced-fit pathway shown previously for the plasma and recombinant wild-type inhibitors (*12*, *26*, *32*, *41*). In this pathway (Scheme 1), heparin interacts weakly with antithrombin in a rapid-equilibrium first step, which induces a conformational change that activates the inhibitor and leads to tighter heparin binding. Analyses at low heparin concentrations indicated that the decrease in affinity caused by the R47H substitution was due both to a lower bimolecular association rate constant, k_{on}, and to a higher dissociation rate constant, k_{off}, for heparin binding. However, the K_d values calculated from these rate constants were somewhat higher than those obtained by equilibrium measurements, in contrast with the corresponding results for both plasma and recombinant antithrombin (*12*, *26*). This discrepancy between the calculated and measured K_d is most likely due to a small contribution of a preequilibrium binding pathway, by which a heparin tetrasaccharide has been shown previously to bind to plasma antithrombin (*41*). In this pathway, the saccharide preferentially binds to a small amount of conformationally activated antithrombin, which in the unbound inhibitor exists in a preequilibrium with native, unactivated antithrombin. The amino acid substitution may have shifted this equilibrium somewhat in favor of the activated form in the R47H/N135A variant. However, the proportion of the activated form can at most be small, as heparin binding caused the normal 35−40% increase of the tryptophan fluorescence of the variant. This increase would have been appreciably lower if a large proportion of the unbound variant had existed in the activated state and thus already had the higher fluorescence characteristic of this state. Similarly, the comparable rate constants for the uncatalyzed inactivation of factor Xa by the R47H/N135A and N135A antithrombin variants indicate that only a small fraction of the R47H/N135A variant can be conformationally activated. Simulations based on a general two-step binding mechanism involving both the induced-fit and preequilibrium pathways (*44*) were done to evaluate the effect of a small contribution by the latter pathway on the parameters derived by assuming that the binding followed only the induced-fit pathway. These simulations showed that such a contribution would result in erroneously high values of k_{off}, in the range expected from the higher K_d, from the intercepts of plots of k_{obs} vs heparin concentration in the concentration range accessible in the stopped-flow analyses.[2] However, they also showed that no other kinetic or equilibrium parameter for the induced-fit mechanism would be detectably affected by this contribution. Values of k_{off} calculated from the measured values of K_d and k_{on} (Table 1) therefore should be accurate. These values are lower than those measured directly, but nevertheless show that the

[2] The erroneously high values of k_{off} are due to the preequilibrium pathway being increasingly favored over the induced-fit pathway as the heparin concentration approaches zero, resulting in the apparent intercept including a contribution from the forward and reverse rate constants for the preequilibrium conformational change (*44*).

decrease in heparin affinity caused by the R47H mutation was due partly to an increased k_{off}.

Extension of the rapid-kinetics studies to high concentrations of the heparin pentasaccharide clarified the background of the decreased k_{on} caused by the R47H substitution. The dissociation equilibrium constant for the first step of the induced-fit binding mechanism (Scheme 1), K_1, was unaffected, showing that Arg47 does not participate in the initial, weak binding of heparin. This initial interaction therefore presumably involves regions of antithrombin some distance away from Arg47. In contrast, the forward rate constant of the second step, k_{+2}, was decreased somewhat by the mutation, indicating that Arg47 is of importance for an optimal rate of the heparin-induced conformational change of antithrombin. Correspondingly, the reverse rate constant of the second step, k_{-2}, was increased by the mutation, as shown by the increased k_{off}, which in the induced-fit binding mechanism is equal to k_{-2}. Arg47 thus also participates in maintaining antithrombin in the activated state by decreasing the rate of reversal of the conformational change and thereby aiding in anchoring the pentasaccharide region of heparin to the inhibitor. These findings are in general agreement with a recent model proposed for the mechanism of pentasacharide binding to antithrombin (*41*). In this model, only the three nonreducing-end saccharide units of the pentasaccharide bind to native, unactivated antithrombin in the initial step and induce the conformational change of the inhibitor in the second step. In contrast, the two reducing-end units just contribute to locking the inhibitor in the activated state by interactions established in the second step. In the crystal structure of the antithrombin−pentasaccharide complex (*22*), Arg47 is shown to interact only with the two saccharide units in the reducing end of the pentasaccharide. Our findings that Arg47 does not participate in the initial binding but is of importance for reducing the rate of reversal of the conformational change are thus in agreement with the proposed binding model. However, the effect of the R47H mutation in decreasing the forward rate of the conformational change suggests that interactions of the reducing-end units of the pentasaccharide with Arg47 may be involved also in the induction of this change.

In conclusion, the results of this work reveal an essential role of Arg47 of antithrombin in heparin binding and only a small contribution of Arg46 to this binding. They also show that Arg47 is not involved in the initial weak step of heparin binding but is of importance for the heparin-induced conformational change. As clinical evidence indicates that the contribution of Arg47 to heparin binding is of physiological significance, these findings should be of importance for design of improved anticoagulant agents based on the structure of the antithrombin-binding pentasaccharide.

ACKNOWLEDGMENT

We thank Yancheng Zuo and Aiqin Lu for production and purification of the antithrombin variants, and Kerstin Nordling for measurements of proteinase inhibition rate constants.

REFERENCES

1. Huber, R., and Carrell, R. W. (1989) *Biochemistry 28*, 8951−8966.
2. Gettins, P. G. W., Patston, P. A., and Olson, S. T. (1996) in *Serpins: Structure, Function and Biology*, R. G. Landes, Austin.
3. Björk, I., and Olson, S. T. (1997) in *Chemistry and Biology of Serpins* (Church, F. C., Cunningham, D. D., Ginsburg, D., Hoffman, M., Stone, S. R., and Tollefsen, D. M., Eds.) pp 17−33, Plenum Press, New York.
4. Olson, S. T., Bock, P. E., Kvassman, J., Shore, J. D., Lawrence, D. A., Ginsburg, D., and Björk, I. (1995) *J. Biol. Chem. 270*, 30007−30017.
5. Lawrence, D. A., Ginsburg, D., Day, D. E., Berkenpas, M. B., Verhamme, I. M., Kvassman, J. O., and Shore, J. D. (1995) *J. Biol. Chem. 270*, 25309−25312.
6. Kvassman, J. O., Verhamme, I., and Shore, J. D. (1998) *Biochemistry 37*, 15491−15502.
7. Stratikos, E., and Gettins, P. G. W. (1997) *Proc. Natl. Acad. Sci. U.S.A. 94*, 453−458.
8. Wilczynska, M., Fa, M., Karolin, J., Ohlsson, P. I., Johansson, L. B.-Å., and Ny, T. (1997) *Nat. Struct. Biol. 4*, 354−357.
9. Stratikos, E., and Gettins, P. G. W. (1998) *J. Biol. Chem. 273*, 15582−15589.
10. Lindahl, U., Bäckström, G., Thunberg, L., and Leder, I. G. (1980) *Proc. Natl. Acad. Sci. U.S.A. 77*, 6551−6555.
11. Choay, J., Petitou, M., Lormeau, J. C., Sinay, P., Casu, B., and Gatti, G. (1983) *Biochem. Biophys. Res. Commun. 116*, 492−499.
12. Olson, S. T., Björk, I., Sheffer, R., Craig, P. A., Shore, J. D., and Choay, J. (1992) *J. Biol. Chem. 267*, 12528−12538.
13. Koide, T., Odani, S., Takahashi, K., Ono, T., and Sakuragawa, N. (1984) *Proc. Natl. Acad. Sci. U.S.A. 81*, 289−293.
14. Owen, M. C., Borg, J. Y., Soria, C., Soria, J., Caen, J., and Carrell, R. W. (1987) *Blood 69*, 1275−1279.
15. Borg, J. Y., Owen, M. C., Soria, C., Soria, J., Caen, J., and Carrell, R. W. (1988) *J. Clin. Invest. 81*, 1292−1296.
16. Gandrille, S., Aiach, M., Lane, D. A., Vidaud, D., Molho-Sabatier, P., Caso, R., de Moerloose, P., Fiessinger, J. N., and Clauser, E. (1990) *J. Biol. Chem. 265*, 18997−19001.
17. Wolf, M., Boyer-Neumann, C., Molho-Sabatier, P., Neumann, C., Meyer, D., and Larrieu, M. J. (1990) *Thromb. Haemostasis 63*, 215−219.
18. Fan, B., Turko, I. V., and Gettins, P. G. W. (1994) *Biochemistry 33*, 14156−14161.
19. Kridel, S. J., Chan, W. W., and Knauer, D. J. (1996) *J. Biol. Chem. 271*, 20935−20941.
20. Ersdal-Badju, E., Lu, A. Q., Zuo, Y. C., Picard, V., and Bock, S. C. (1997) *J. Biol. Chem. 272*, 19393−19400.
21. Lane, D. A., Bayston, T., Olds, R. J., Fitches, A. C., Cooper, D. N., Millar, D. S., Jochmans, K., Perry, D. J., Okajima, K., Thein, S. L., and Emmerich, J. (1997) *Thromb. Haemostasis 77*, 197−211.
22. Jin, L., Abrahams, J. P., Skinner, R., Petitou, M., Pike, R. N., and Carrell, R. W. (1997) *Proc. Natl. Acad. Sci. U.S.A. 94*, 14683−14688.
23. van Boeckel, C. A. A., Grootenhuis, P. D. J., and Visser, A. (1994) *Nat. Struct. Biol. 1*, 423−425.
24. Huntington, J. A., Olson, S. T., Fan, B. Q., and Gettins, P. G. W. (1996) *Biochemistry 35*, 8495−8503.
25. Ersdal-Badju, E., Lu, A., Peng, X., Picard, V., Zendehrouh, P., Turk, B., Björk, I., Olson, S. T., and Bock, S. C. (1995) *Biochem. J. 310*, 323−330.
26. Turk, B., Brieditis, I., Bock, S. C., Olson, S. T., and Björk, I. (1997) *Biochemistry 36*, 6682−6691.
27. Olson, S. T., Frances-Chmura, A. M., Swanson, R., Björk, I., and Zettlmeissl, G. (1997) *Arch. Biochem. Biophys. 341*, 212−221.
28. Olson, S. T., and Björk, I. (1991) *J. Biol. Chem. 266*, 6353−6364.
29. Olson, S. T., Björk, I., and Shore, J. D. (1993) *Methods Enzymol. 222*, 525−560.
30. Nordenman, B., Danielsson, Å., and Björk, I. (1978) *Eur. J. Biochem. 90*, 1−6.
31. Olson, S. T., and Shore, J. D. (1981) *J. Biol. Chem. 256*, 11065−11072.

32. Olson, S. T., Srinivasan, K. R., Björk, I., and Shore, J. D. (1981) *J. Biol. Chem. 256*, 11073−11079.
33. Brennan, S. O., George, P. M., and Jordan, R. E. (1987) *FEBS Lett. 219*, 431−436.
34. Björk, I., Ylinenjärvi, K., Olson, S. T., Hermentin, P., Conradt, H. S., and Zettlmeissl, G. (1992) *Biochem. J. 286*, 793−800.
35. Turko, I. V., Fan, B., and Gettins, P. G. W. (1993) *FEBS Lett. 335*, 9−12.
36. Picard, V., Ersdal-Badju, E., and Bock, S. C. (1995) *Biochemistry 34*, 8433−8440.
37. Carrell, R. W., Stein, P. E., Fermi, G., and Wardell, M. R. (1994) *Structure 2*, 257−270.
38. Wardell, M. R., Chang, W. S. W., Bruce, D., Skinner, R., Lesk, A. M., and Carrell, R. W. (1997) *Biochemistry 36*, 13133−13142.
39. Björk, I., and Fish, W. W. (1982) *J. Biol. Chem. 257*, 9487−9493.
40. Record, M. T., Jr., Lohman, T. M., and de Haseth, P. (1976) *J. Mol. Biol. 107*, 145−158.
41. Desai, U. R., Petitou, M., Björk, I., and Olson, S. T. (1998) *J. Biol. Chem. 273*, 7478- 7487.
42. Brunel, F., Duchange, N., Fischer, A. M., Cohen, G. N., and Zakin, M. M. (1987) *Am. J. Hematol. 25*, 223−224.
43. Meagher, J. L., Huntington, J. A., Fan, B. Q., and Gettins, P. G. W. (1996) *J. Biol. Chem. 271*, 29353−29358.
44. Lindahl, P., Raub-Segall, E., Olson, S. T., and Björk, I. (1991) *Biochem. J. 276*, 387−394.

BI990686B